JOC Article
pubs.acs.org/joc

Lower Rim 1,3-Di{bis(2-picolyl)}amide Derivative of Calix[4]arene (L) as Ratiometric Primary Sensor toward Ag^+ and the Complex of Ag^+ as Secondary Sensor toward Cys: Experimental, Computational, and Microscopy Studies and INHIBIT Logic Gate Properties of L‡

Roymon Joseph, Balaji Ramanujam, Amitabha Acharya, and Chebrolu P. Rao*

Bioinorganic Laboratory, Department of Chemistry, Indian Institute of Technology Bombay, Mumbai 400 076, India

cprao@iitb.ac.in

Received July 31, 2009

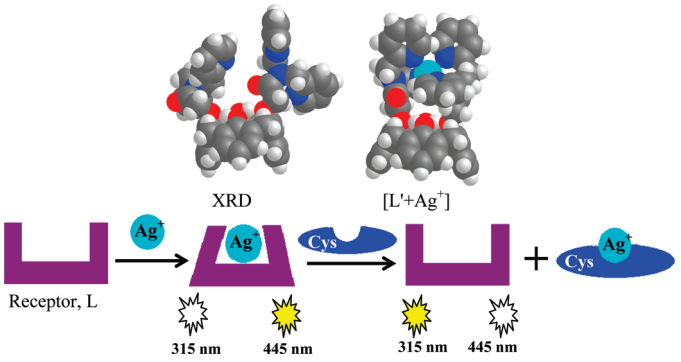

A structurally characterized lower rim 1,3-di{bis(2-picolyl)}amide derivative of calix[4]arene (L) exhibits high selectivity toward Ag^+ by forming a 1:1 complex, among nine other biologically important metal ions, *viz*., Na^+, K^+, Mg^{2+}, Ca^{2+}, Mn^{2+}, Fe^{2+}, Co^{2+}, Ni^{2+}, and Zn^{2+}, as studied by fluorescence, absorption, and ^1H NMR spectroscopy. The 1:1 complex formed between L and Ag^+ has been further proven on the basis of ESI mass spectrometry and has been shown to have an association constant, K_a, of $11117 \pm 190\ M^{-1}$ based on fluorescence data. L acts as a primary ratiometric sensor toward Ag^+ by *switch-on* fluorescence and exhibits a lowest detectable concentration of 450 ppb. DFT computational studies carried out in mimicking the formation of a 1:1 complex between L and Ag^+ resulted in a tetrahedral complex wherein the nitrogens of all four pyridyl moieties present on both arms are being coordinated. Whereas these pyridyls are located farther apart in the crystal structure, appropriate dihedral changes are induced in the arms in the presence of silver ion in order to form a coordination complex. Even the nanostructural features obtained in TEM clearly differentiates L from its Ag^+ complex. The *in situ* prepared silver complex of L detects Cys ratiometrically among the naturally occurring amino acids to a lowest concentration of 514 ppb by releasing L from the complex followed by formation of the cysteine complex of Ag^+. These were demonstrated on the basis of emission, absorption, ^1H NMR, and ESI mass spectra. The INH logic gate has also been generated by choosing Ag^+ and Cys as input and by monitoring the output signal at 445 nm that originates from the excimer emission of L in the presence of Ag^+. Thus L is a potential primary sensor toward Ag^+ and is a secondary sensor toward Cys.

Introduction

Recognition of metal ions and amino acids are of prime interest in the context of metalloproteins and metalloenzymes, where Ag^+ and Cys are not exceptions. Though the Ag^+ is not a biologically essential element, its complexes are used in medicine and agriculture.[1] The antimicrobial

‡ Dedicated to Professor Padmanabhan Balaram on the occasion of his 60th birthday.

(1) (a) Jung, W. K.; Koo, H. C.; Kim, K. W.; Shin, S.; Kim, S. H.; Park, Y. H. *Appl. Environ. Microbiol.* **2008**, *74*, 2171. (b) Silver, S.; Phung, L. T.; Silver, G. *J. Ind. Microbiol. Biotechnol.* **2006**, *33*, 627.

DOI: 10.1021/jo901676s Published on Web 10/09/2009

action of silver mainly takes place through its interactions with sulfur in the case of amino acids and peptides,[2] and Ag^+ ions are inactive toward other amino acids. A side effect of silver originating from its prolonged use is irreversible darkening of the skin and mucous membrane.[3] Accumulation of silver by microbial species could also act as a source for this element.[4] Among the 20 naturally occurring amino acids, Cys plays an important role in living cells.[5] Both the deficiency and excess accumulation of Cys are detrimental to life.[6] Therefore, the detection and sensing of silver and Cys, by a single molecular system with dual functionality, are certainly challenging and are intriguing to the current researchers. Owing to the ubiquitous nature of calix[4]arenes[7] by possessing hydrophilic and hydrophobic characters together in the same structure, these molecules can act as good mimics of enzymes[8] and also provide a suitable platform for building appropriate binding cores. There are some reports in the literature for the selective recognition of silver either by potentiometry,[9] by ^{1}H NMR,[10] or by fluorescence technique[11] using calix[4]arene derivatives. Similarly, amino acid recognition by calix[4]arene derivatives is rather limited, and the recognitions were mainly carried out by mass spectroscopy,[12] calorimetry,[13] ^{1}H NMR studies,[13b,c,14] and HPLC;[15] detection by fluorescence spectroscopy[16] is scarce. Coleman et al. reported several *p*-sulfonatocalix[4]arenes for amino acid recognition and were able to establish the structure of these calixarene amino acid complexes even in the solid state.[17] There are few reports available in the literature in which amino acid recognition was achieved by chemo sensing ensemble.[12b,18] Though there are several receptors to recognize Ag^+ and Cys individually, to the best of our knowledge, there has been no report of any calix[4]arene molecular system that would detect selectively Ag^+ followed by Cys by acting as primary as well as secondary sensor. Thus the present paper reports the synthesis, characterization, and ratiometric silver-sensing properties of a lower rim functionalized calix[4]arene possessing dipicolyl moiety connected through an amide linkage (L) and the recognition of Cys by the corresponding silver complex. Thus L acts as a primary sensor toward Ag^+ and as a secondary sensor toward Cys and thereby exhibits INH logic gate properties. The sensor property of L toward Ag^+ has been proven to be due to the formation of the complex on the basis of different experimental and computational studies. Experimental evidence has also been provided for the release of L from the reaction of Cys with the silver complex.

Results and Discussion

Receptor Molecule L. The receptor molecule, L, has been synthesized by four known steps starting from *p*-*tert*-butyl calix[4]arene as given in Scheme 1,[19] (see also Experimental Section). The acid chloride derivative **4** was prepared by reacting **3** with $SOCl_2$, followed by coupling with bis(2-picolyl)-amine to result in the receptor molecule, L. All of these molecules including L were characterized satisfactorily by ^{1}H NMR, ^{13}C NMR, ESI MS, FTIR, and elemental analysis. The cone conformation of L has been confirmed by ^{1}H NMR spectroscopy and also by the structure determined on the basis of single crystal X-ray diffraction, as reported in this paper.

Crystal Structure of L. The ligand L was crystallized by slow diffusion of diethyl ether into a solution containing L in a mixture of methanol and chloroform, and the structure was determined by single crystal XRD (Supporting Information, S01).

(2) Mcdonnell, G.; Russell, D. A. *Clin. Microbiol. Rev.* **1999**, *12*, 147.
(3) (a) Butkus, M. A.; Labare, M. P.; Starke, J. A.; Moon, K.; Talbot, M. *Appl. Environ. Microbiol.* **2004**, *70*, 2848. (b) Petering, H. G. *Pharmaolc. Ther. A* **1976**, *1*, 127. (c) Russell, A. D.; Hugo, W. B. *Prog. Med. Chem.* **1994**, *31*, 351.
(4) Slawson, R. M.; Van Dyke, M. I.; Lee, H.; Trevors, J. T. *Plasmid* **1992**, *27*, 72.
(5) (a) Ball, R. O.; Courtney-Martin, G.; Pencharz, P. B. *J. Nutr.* **2006**, *136*, 1682S. (b) Griffith, W. *Method Enzymol.* **1987**, *143*, 366.
(6) (a) Shahrokhian, S. *Anal. Chem.* **2001**, *73*, 5972. (b) Heafield, M. T.; Fearn, S.; Steventon, G. B.; Waring, R. H.; Williams, A. C.; Sturman, S. G. *Neurosci. Lett.* **1990**, *110*, 216. (c) Puka-Sundvall, M.; Eriksson, P.; Nilsson, M.; Sandberg, M.; Lehmann, A. *Brain Res.* **1995**, *705*, 65.
(7) (a) Gutsche, C. D. *Acc. Chem. Res.* **1983**, *16*, 161. (b) Shinkai, S. *Tetrahedron* **1993**, *49*, 8933.
(8) (a) Izzet, G.; Douziech, B.; Prange, T.; Tomas, A.; Jabin, I.; Mest, Y. L.; Reinaud, O. *Proc. Natl. Acad. Sci. U.S.A.* **2005**, *102*, 6831. (b) Rondelez, Y.; Bertho, G.; Reinaud, O. *Angew. Chem., Int. Ed.* **2002**, *41*, 1044. (c) Cacciapaglia, R.; Casnati, A.; Mandolini, L.; Reinhoudt, D. N.; Salvio, R.; Sartori, A.; Ungaro, R. *J. Am. Chem. Soc.* **2006**, *128*, 12322. (d) Molenveld, P.; Engbersen, J. F. J.; Reinhoudt, D. N. *J. Org. Chem.* **1999**, *64*, 6337. (e) Molenveld, P.; Stikvoort, W. M. G.; Kooijman, H.; Spek, A. L.; Engbersen, J. F. J.; Reinhoudt, D. N. *J. Org. Chem.* **1999**, *64*, 3896. (f) Molenveld, P.; Engbersen, J. F. J.; Reinhoudt, D. N. *Angew. Chem., Int. Ed.* **1999**, *38*, 3189.
(9) (a) Kumar, M.; Mahajan, R. K.; Sharma, V.; Singh, H.; Sharma, N.; Kaur, I. *Tetrahedron Lett.* **2001**, *42*, 5315. (b) Zeng, X.; Weng, L.; Chen, L.; Leng, X.; Zhang, Z.; He, X. *Tetrahedron Lett.* **2000**, *41*, 4917. (c) Zeng, X.; Weng, L.; Chen, L.; Leng, X.; Ju, H.; He, X.; Zhang, Z.-Z. *J. Chem. Soc., Perkin Trans. 2* **2001**, 545.
(10) (a) Creaven, B. S.; Deasy, M.; Flood, P. M.; McGinley, J.; Murray, B. A. *Inorg. Chem. Commun.* **2008**, *11*, 1215. (b) Wong, M. S.; Xia, P. F.; Zhang, X. L.; Lo, P. K.; Cheng, Y.-K.; Yeung, K.-T.; Guo, X.; Shuang, S. *J. Org. Chem.* **2005**, *70*, 2816. (c) Struck, O.; Chrisstoffels, L. A. J.; Lugtenberg, R. J. W.; Verboom, W.; van Hummel, G. J.; Harkema, S.; Reinhoudt, D. N. *J. Org. Chem.* **1997**, *62*, 2487. (d) Kim, S. K.; Lee, J. K.; Lee, S. H.; Lim, M. S.; Lee, S. W.; Sim, W.; Kim, J. S. *J. Org. Chem.* **2004**, *69*, 2877. (e) Wong, M. S.; Xia, P. F.; Lo, P. K.; Sun, X. H.; Wong, W. Y.; Shuang, S. *J. Org. Chem.* **2006**, *71*, 940. (f) Zeng, X.; Sun, H.; Chen, L.; Leng, X.; Xu, F.; Li, Q.; He, X.; Zhang, W.; Zhang, Z.-Z. *Org. Biomol. Chem.* **2003**, *1*, 1073. (g) Kim, J. S.; Yang, S. H.; Rim, J. A.; Kim, J. Y.; Vicens, J.; Shinkai, S. *Tetrahedron Lett.* **2001**, *42*, 8047. (h) Budka, J.; Lhotak, P.; Stibor, I.; Michlova, V.; Sykora, J.; Cisarova, I. *Tetrahedron Lett.* **2002**, *43*, 2857.
(11) Kim, J. S.; Noh, K. H.; Lee, S. H.; Kim, S. K.; Kim, S. K.; Yoon, J. *J. Org. Chem.* **2003**, *68*, 597.
(12) (a) Stone, M. M.; Franz, A. H.; Lebrilla, C. B. *J. Am. Soc. Mass Spectrom.* **2002**, *13*, 964. (b) Perret, F.; Morel-Desrosiers, N.; Coleman, A. W. *J. Supramol. Chem.* **2002**, *2*, 533.
(13) (a) Zielenkiewicz, W.; Marcinowicz, A.; Cherenok, S.; Kalchenko, V. I.; Poznanski, J. *Supramol. Chem.* **2006**, *18*, 167. (b) Arena, G.; Casnati, A.; Contino, A.; Magri, A.; Sansone, F.; Sciotto, D.; Ungaro, R. *Org. Biomol. Chem.* **2006**, *4*, 243. (c) Douteau-Guével, N.; Perret, F.; Coleman, A. W.; Morel, J.-P.; Morel-Desrosiers, N. *J. Chem. Soc., Perkin Trans. 2* **2002**, 524. (d) Douteau-Guével, N.; Coleman, A. W.; Morel, J.-P. ; Morel-Desrosiers, N. *J. Chem. Soc., Perkin Trans. 2* **1999**, 629.
(14) (a) Douteau-Guevel, N.; Coleman, A. W.; Morel, J.-P.; Morel-Desrosiers, N. *J. Phys. Org. Chem.* **1998**, *11*, 693. (b) Da Silva, E.; Coleman, A. W. *Tetrahedron* **2003**, *59*, 7357. (c) Arena, G.; Contino, A.; Gulino, F. G.; Magri, A.; Sansone, F.; Sciotto, D.; Ungaro, R. *Tetrahedron Lett.* **1999**, *40*, 1597. (d) Frish, L.; Sansone, F.; Casnati, A.; Ungaro, R.; Cohen, Y. *J. Org. Chem.* **2000**, *65*, 5026. (e) Casnati, A.; Fabbi, M.; Pelizzi, N.; Pochini, A.; Sansone, F.; Ungaro, R. *Bioorg. Med. Chem. Lett.* **1996**, *6*, 2699. (f) Baldini, L.; Casnati, L.; Sansone, F.; Ungaro, R. *Chem. Soc. Rev.* **2007**, *36*, 254. (g) Ikeda, A.; Shinkai, S. *Chem. Rev.* **1997**, *97*, 1713. (e) Casnati, A.; Sansone, F.; Ungaro, R. *Acc. Chem. Res.* **2003**, *36*, 246.
(15) Kalchenko, O. I.; Da Silva, E.; Coleman, A. W. *J. Inclusion Phenom. Macrocyclic Chem.* **2002**, *43*, 305.
(16) (a) Lu, J. Q.; Zhang, L.; Sun, T. Q.; Wang, G. X.; Wu, L. Y. *Chin. Chem. Lett.* **2006**, *17*, 575. (b) Li, H.; Wang, X. *Photochem. Photobiol. Sci.* **2008**, *7*, 694.
(17) (a) Perret, F.; Lazar, A. N.; Coleman, A. W. *Chem. Commun.* **2006**, 2425. (b) Selkti, M.; Coleman, A. W.; Nicolis, I.; Douteau-Guével, N.; Villain, F.; Tomas, A.; de Rango, C. *Chem. Commun.* **2000**, 161. (c) Lazar, A. N.; Danylyuk, O.; Suwinska, K.; Coleman, A. W. *J. Mol. Struct.* **2006**, *825*, 20.
(18) Ait-Haddou, H.; Wiskur, S. L.; Lynch, V. M.; Anslyn, E. V. *J. Am. Chem. Soc.* **2001**, *123*, 11296.
(19) Joseph, R.; Ramanujam, B.; Acharya, A.; Rao, C. P. *Tetrahedron Lett.* **2009**, *50*, 2735.

SCHEME 1. Synthesis of Lower Rim Calix[4]arene-1,3-di-derivatives, L, and Its XRD Structure[a]

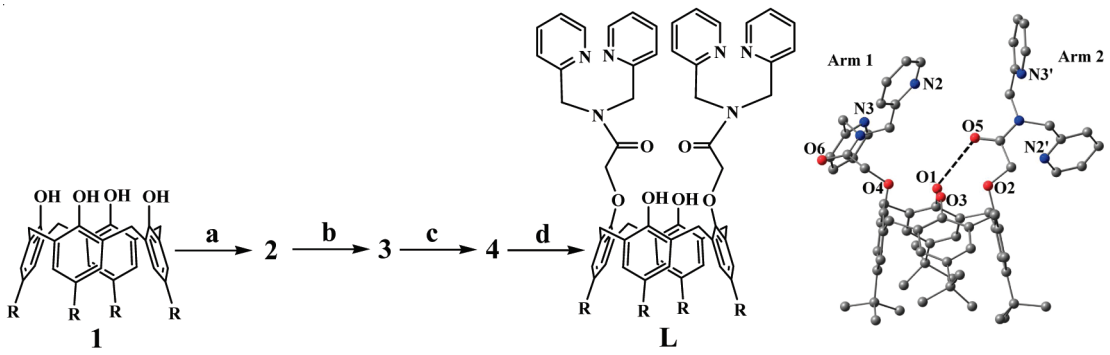

[a]Reagents and conditions: (a) bromoethylacetate/K_2CO_3/acetone; (b) NaOH/C_2H_5OH, reflux; (c) $SOCl_2$/benzene, reflux; (d) bis(2-picolyl)amine/Et_3N/THF. R = *tert*-butyl.

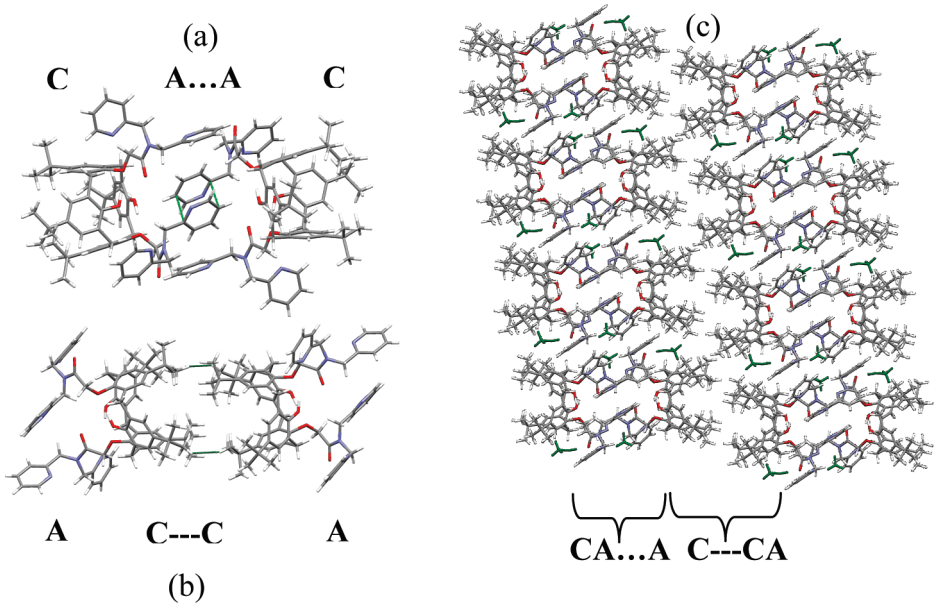

FIGURE 1. From the crystal structure of L: (a) dimer formed by the arms of L (i.e., CA···AC type), (b) dimer formed by the hydrophobic arene cavity (i.e., AC---CA type), and (c) lattice structure of L where methanols are shown in green. "A" is the arms portion, and "C" is the arene cavity.

In the asymmetric unit cell of the centrosymmetric triclinic system, two methanol molecules were crystallized along with one molecule of L. The two O−H···O intramolecular hydrogen bonds {H···O, O···O distances (Å) and O−H···O angle (deg) are 1.820, 2.844, 169 and 2.014, 2.784, 147} observed at the lower rim fixes the calix[4]arene in a cone conformation. Because of the presence of a hydrogen bond between amide CO and phenolic OH (2.362 Å, 3.010 Å, 131°), one of the amide CO is projected inside the cavity of calix[4]arene (Arm 2, Scheme 1), while lack of the hydrogen bonding makes the other amide CO to point outside the calix[4]arene cavity (Arm 1, Scheme 1). The nitrogen atoms present in the pyridyl moiety generates possible binding cores in L (based on arms, N_4 and N_4O_2; arms + phenolic OH, O_4 and N_4O_6). Among these, the nitrogen-rich pyridyl core is best suited for transition metal ions.[19,20] The details of the structure determination and the refinement as well as some important bond lengths, bond angles, and hydrogen bond data are given in Supporting Information, S01. However, the two arms are disposed in space farther apart by exhibiting inter-arm N···N distances ranging from 5.1 to 8.9 Å and intra-arm N···N distances ranging from 4.9 to 5.4 Å. Hence, L needs to undergo some conformational changes if the arms are to be involved in binding to a metal ion through coordination.

Lattice Structure. In the lattice, L forms a dimer through the interactions extended between the arms of both partners in a head-to-head fashion. These are through $\pi-\pi$ interactions extended between the pyridyl moieties of similar type of arms of the two partners (Figure 1a). Such head-to-head dimers form a supramolecular column through arene−arene interactions extended between the hydrophobic cavities of the two neighbor dimers via the *tert*-butyl groups, where the shortest distance between the *tert*-butyl carbons being ~3.45 Å (Figure 1b). Thus the column is a repetition of ---CA···AC---CA···AC---CA···AC---CA···, where "C" represents the hydrophobic cavity portion possessing the *tert*-butyl groups and "A" represents the arms portion. These columns are further connected through weak H-bond

(20) Joseph, R.; Ramanujam, B.; Pal, H.; Rao, C. P. *Tetrahedron Lett.* **2008**, *49*, 6257.

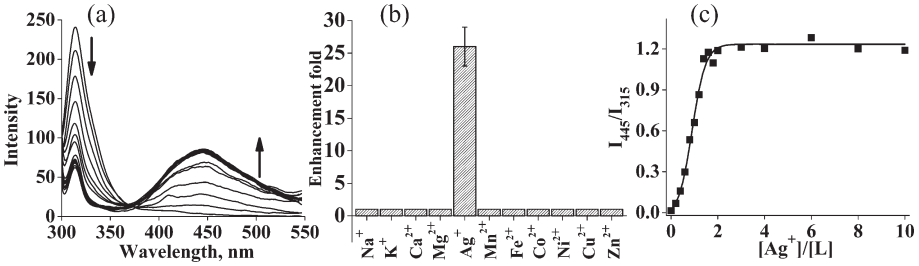

FIGURE 2. (a) Fluorescence spectral traces of L (10 μM) during titration with Ag^+; (b) histogram representing the relative fluorescence intensity (I/I_0) observed at 445 nm; (c) plot of relative fluorescence intensity ratio, *viz*., I_{445}/I_{315} vs [Ag^+]/[L] mole ratio.

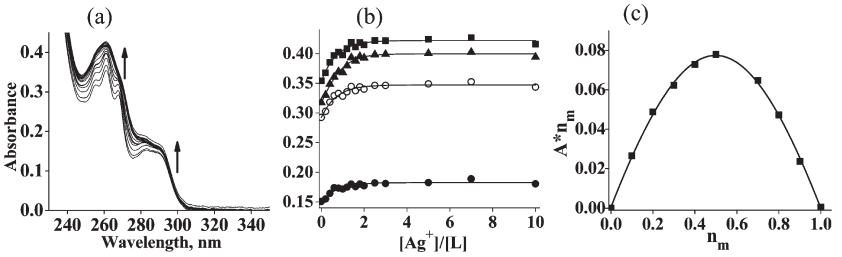

FIGURE 3. Absorption spectral titration of L with Ag^+: (a) spectral traces observed during the titration in the region 230−350 nm; (b) plots of absorbance versus mole ratio of [Ag^+]/[L] for different bands (● = 282, ○ = 268, ■ = 261, and ▲ = 255 nm); and (c) Job's plot of n_m versus A^*n_m, where n_m is the mole fraction of the metal ion added and A is the absorbance.

interactions offered by the solvent methanol molecules present in the lattice resulting in the structure shown in Figure 1c.

A. Primary Sensor Properties of L in the Selective Recognition of Ag^+. Fluorescence Titration Studies. Calix[4]arene derivative L has been studied for its interaction with Ag^+ by exciting the solutions at 285 nm and by following the emission bands observed at 315 and 445 nm, which shows fluorescence quenching and enhancement, respectively, as the concentration of added Ag^+ increases. This resulted in the formation of an iso-emissive point at 375 nm (Figure 2a). Moreover the ligand L showed a fluorescence enhancement of ~25-fold during the titration with Ag^+ (Figure 2b). None of the other M^{n+} ions, *viz*., Na^+, K^+, Mg^{2+}, Ca^{2+}, Mn^{2+}, Fe^{2+}, Co^{2+}, Ni^{2+}, Cu^{2+}, and Zn^{2+}, showed fluorescence changes except Cu^{2+}, which shows changes only in the 315 nm band, suggesting that the changes observed in this band alone can be used for selective recognition of Cu^{2+} as reported by us recently,[19] while Ag^+ can be selectively recognized by ratiometric variation of the fluorescence intensity, *viz*., [I_{445}/I_{315}] as reported in this paper (Figure 2c). The new emission band at 445 nm originates from the excimer formation of pyridyl moieties in the excited state, suggesting that the silver ion brings the pyridyl moieties together during the metal ion binding. Such excimer formation has been reported in the literature for a tetra-derivative of calix[4]arene containing pyridyl moieties at its lower rim.[21] The binding constant of L with Ag^+ was calculated by the Benesi−Hildebrand equation, and the corresponding association constant K_a was found to be 11117 ± 190 M^{-1}. The minimum concentration at which L can detect Ag^+ has been found to be 450 ppb (Supporting Information, S02).

Absorption Titration Studies. To get further support for the metal ion binding, absorption titration has also been carried out between L and Ag^+. The ligand L exhibited four absorption bands centered at 261, 285, 255, and 268 nm; all of these bands showed an increase in the absorbance upon addition of Ag^+ (Figure 3a); and saturation in absorbance was observed at ≥2 equiv (Figure 3b). The stoichiometry of the complex formed between L and Ag^+ has been derived to be 1:1 on the basis of a Job's plot (Figure 3c), and the K_a value was found to be 11941 M^{-1}.

Electrospray Mass Spectrometry. ESI MS spectrum obtained during the titration of L with Ag^+ results in a 100% molecular ion peak at m/z = 1235.5 corresponding to a 1:1 complex. The isotopic peak pattern observed for Ag^+ closely resembles that of the calculated one, supporting the presence of metal ion and hence the complex formation (Figure 4).

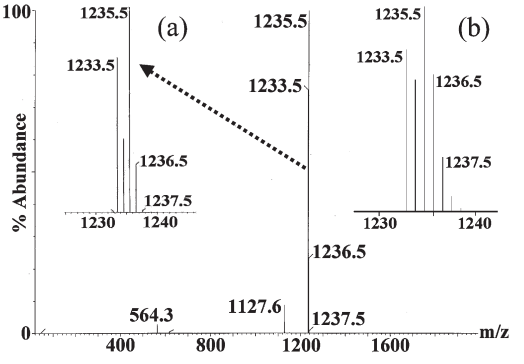

FIGURE 4. ESI MS spectrum obtained in the titration of L with Ag^+. Insets: (a) expanded peak of the complex; (b) calculated isotopic pattern for the complex of [L+Ag^+].

^{1}H NMR Titration of L with Ag^+. Interaction between L and Ag^+ was studied by NMR spectroscopy in DMSO-d_6. During the titration, the concentration of L was kept constant and the added [Ag^+] mole ratio was varied, *viz*., 0.5, 1, 1.5, 2.0, 2.5, 3.5,

(21) Souchon, V.; Maisonneuve, S.; David, O.; Leray, I.; Xie, J.; Valeur, B. *Photochem. Photobiol. Sci.* **2008**, *7*, 1323.

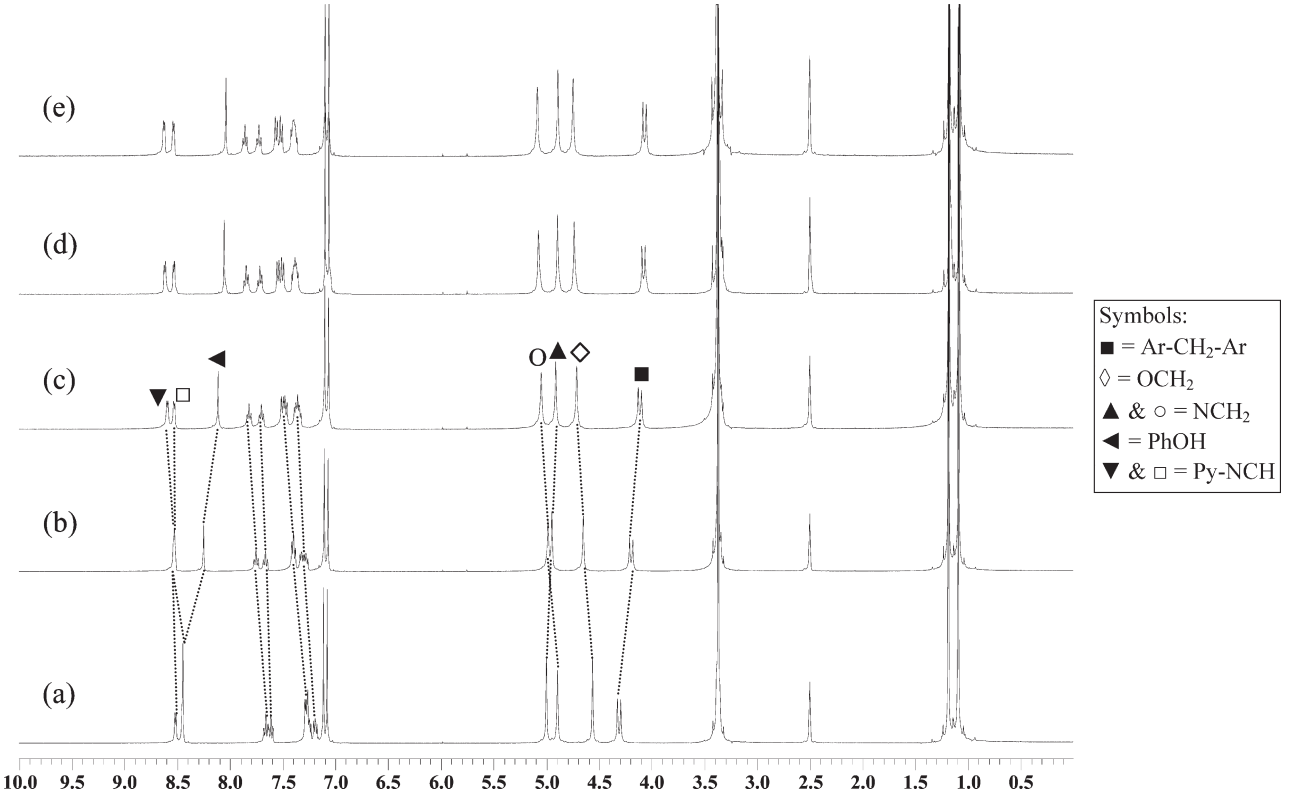

FIGURE 5. ^{1}H NMR spectra measured during the titration of L with different mole ratios of Ag^+ (in DMSO-d_6): (a) 0; (b) 0.5; (c) 1.0; (d) 1.5; (e) 2.0.

and 4.5 equiv (Figure 5). ^{1}H NMR studies showed minimal to marginal changes in the δ values of pyridyl, phenolic-OH, and bridged -CH_2 protons (Figure 6). Absence of any changes observed in the chemical shift of aromatic and/or *tert*-butyl protons rules out any interaction between the arene and Ag^+. If the Ag^+ were to be interacting with the arene cavity of the calixarene, the aromatic protons would show corresponding shifts as reported in the literature by Shinkai and co-workers.[22] The downfield shift observed in the pyridyl and the arm -NCH_2 protons is suggestive of the binding of Ag^+ in the pyridyl core through nitrogens. The upfield shift observed in the bridged -CH_2 and the phenolic -OH groups of calix[4]arene are suggestive of the breakage and/or weakening of lower rim H-bond interactions to result in conformational changes as reported for calix[4]arene derivatives in the literature in the presence of Ag^+ ion[10f] (Figure 6).

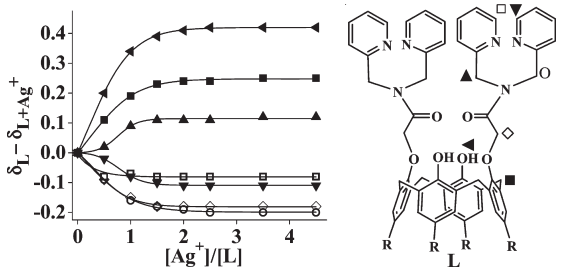

FIGURE 6. Metal-ion-induced shift ($\Delta\delta = \delta_L - \delta_{L+Ag^+}$) observed with different protons of L at various mole ratios of $[Ag^+]/[L]$ as taken from Figure 5. Symbols are the same as in Figure. 5.

(22) Ikeda, A.; Tsuzuki, H.; Shinkai, S. *J. Chem. Soc., Perkin Trans. 2* **1994**, 2073.

Competitive Metal Ion Titrations. To find out whether L can detect Ag^+ selectively even in the presence of other metal ions, competitive metal ion titrations were carried out. A 1:5 mole ratio mixture of L and M^{n+} were titrated against different equivalents of Ag^+, and the corresponding fluorescence emission spectra were recorded. It was found that Ag^+ can replace all the other M^{n+} ions except Cu^{2+}, as can be seen from Figure 7. Thus, while Ag^+ ion can be detected quantitatively in the presence of a number of biologically relevant M^{n+} ions except Cu^{2+}, the Cu^{2+} indeed can be quantified by L in the presence of all of these.

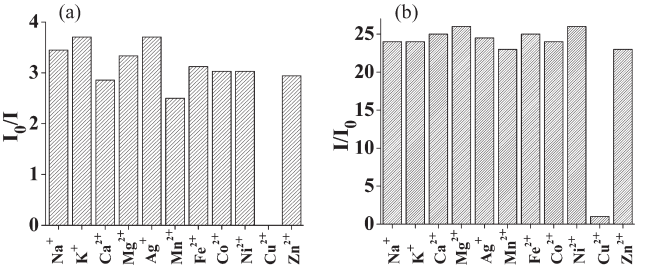

FIGURE 7. Relative fluorescence intensity of L upon addition of 3 equiv of Ag^+ in the presence of 5 equiv of M^{n+} ions at (a) 315 and (b) 445 nm.

Control Molecules. To substantiate the role of the calix[4]arene platform and the presence of a nitrogen core in the recognition process of L, several related molecular systems, *viz*., L_1, L_2, L_3, and L_4, shown in Figure 8 have been subjected to similar titration studies by emission spectroscopy. These were chosen for the following reasons: (a) L_1

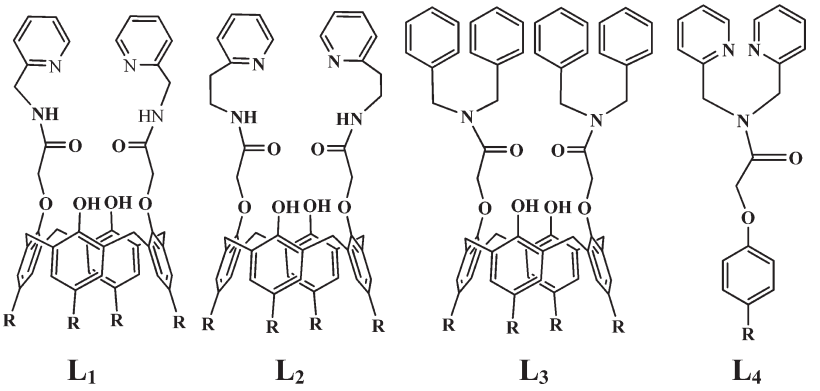

FIGURE 8. Schematic representation of the control molecules, L_1, L_2, L_3, and L_4. R = *tert*-butyl.

contains one methyl pyridyl moiety instead of the two present in L; (b) the binding core present in L_2 has one additional CH_2 group but one less pyridyl group, providing a different binding core compared to that of L; (c) the pyridyl moieties in L have been replaced by noncoordinating benzyl moieties in L_3; (d) the calix[4]arene platform present in L has been replaced by a single strand in L_4 while retaining the binding arm.

Synthesis and characterization details of the control molecules, L_1 and L_3, have been discussed by us earlier.[19] L_2 was prepared by coupling a diacid chloride derivative of calix[4]arene, **4** (given in Scheme 1), with 2-amino ethyl pyridine, and the product formed was purified and characterized by spectral techniques (Supporting Information, S03). A single strand derivative having *p-tert*-butyl phenol instead of calix[4]arene has been synthesized by coupling the acid chloride derivative of *p-tert*-butyl phenol with bis(2-picolyl)amine moiety as shown in Scheme 2 (Supporting Information, S03). The product formed has been purified by silica gel

SCHEME 2. Synthesis of L_4[a]

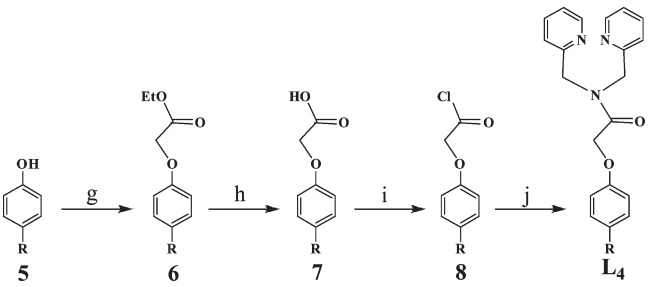

[a]Reagents and conditions: (g) bromoethylacetate/K_2CO_3/acetone; (h) KOH/C_2H_5OH/water, reflux; (i) $SOCl_2$/benzene, reflux; and (j) bis(2-picolyl)amine/Et_3N/THF. R = *tert*-butyl.

column chromatography and was characterized by different analytical and spectral techniques.

The control molecules, L_1, L_2, L_3, and L_4, have been studied for their binding ability toward Ag^+ ion, and it was found that none of these show any fluorescence change, indicating their noninteractive nature with Ag^+ ion (Figure 9).

Computational Modeling of the Ag^+ Complex of L. As the stiochiometry of the complex formed between Ag^+ and L was found to be 1:1 based on emission, absorption, and ESI

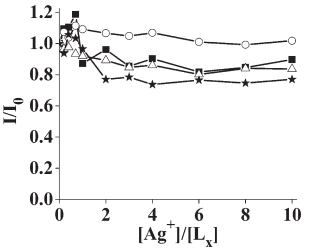

FIGURE 9. Plot of relative fluorescence intensity (I/I_0) versus mole ratio of Ag^+ added to the control molecules: L_1 (■), L_2 (Δ), L_3 (○), and L_4 (★).

MS studies, the nature of Ag^+ coordination with L was studied by computational studies using the Gaussian03 software package.[23] The initial geometry for L was taken from the single crystal XRD structure. As the number of atoms present in L was too large, L′ was generated from L by replacing the *tert*-butyl groups present at the upper rim with hydrogens. Such changes made in calixarene systems to reduce the computational times exhibited no influence on the conformation of the arm as shown by us earlier.[20,24] L′ is chemically and structurally similar to L and hence was used in the calculations to reduce the computational times. The geometry optimizations for L and L′ were done in a cascade fashion starting from semiempirical PM3 followed by *ab initio* HF to DFT B3LYP by using various basis sets, *viz*., PM3 → HF/STO-3G → HF/3-21G → HF/6-31G → B3LYP/STO-3G → B3LYP/3-21G → B3LYP/6-31G. The optimization at the DFT level showed considerable change in the dihedral angles of the arms when

(23) Frisch, M. J.; Trucks, G. W.; Schlegel, H. B.; Scuseria, G. E.; Robb, M. A.; Cheeseman, J. R.; Montgomery, J. A., Jr.; Vreven, T.; Kudin, K. N.; Burant, J. C.; Millam, J. M.; Iyengar, S. S.; Tomasi, J.; Barone, V.; Mennucci, B.; Cossi, M.; Scalmani, G.; Rega, N.; Petersson, G. A.; Nakatsuji, H.; Hada, M.; Ehara, M.; Toyota, K.; Fukuda, R.; Hasegawa, J.; Ishida, M.; Nakajima, T.; Honda, Y.; Kitao, O.; Nakai, H.; Klene, M.; Li, X.; Knox, J. E.; Hratchian, H. P.; Cross, J. B.; Adamo, C.; Jaramillo, J.; Gomperts, R.; Stratmann, R. E.; Yazyev, O.; Austin, A. J.; Cammi, R.; Pomelli, C.; Ochterski, J. W.; Ayala, P. Y.; Morokuma, K.; Voth, G. A.; Salvador, P.; Dannenberg, J. J.; Zakrzewski, V. G.; Dapprich, S.; Daniels, A. D.; Strain, M. C.; Farkas, O.; Malick, D. K.; Rabuck, A. D.; Raghavachari, K.; Foresman, J. B.; Ortiz, J. V.; Cui, Q.; Baboul, A. G.; Clifford, S.; Cioslowski, J.; Stefanov, B. B.; Liu, G.; Liashenko, A.; Piskorz, P.; Komaromi, I.; Martin, R. L.; Fox, D. J.; Keith, T.; Al-Laham, M. A.; Peng, C. Y.; Nanayakkara, A.; Challacombe, M.; Gill, P. M.W.; Johnson, B.; Chen, W.; Wong, M. W.; Gonzalez, C.; Pople, J. A. *Gaussian 03, revision C.02*; Gaussian, Inc.: Wallingford, CT, 2004.

(24) Joseph, R.; Ramanujam, B.; Acharya, A.; Khutia, A.; Rao, C. P. *J. Org. Chem.* **2008**, *73*, 5745.

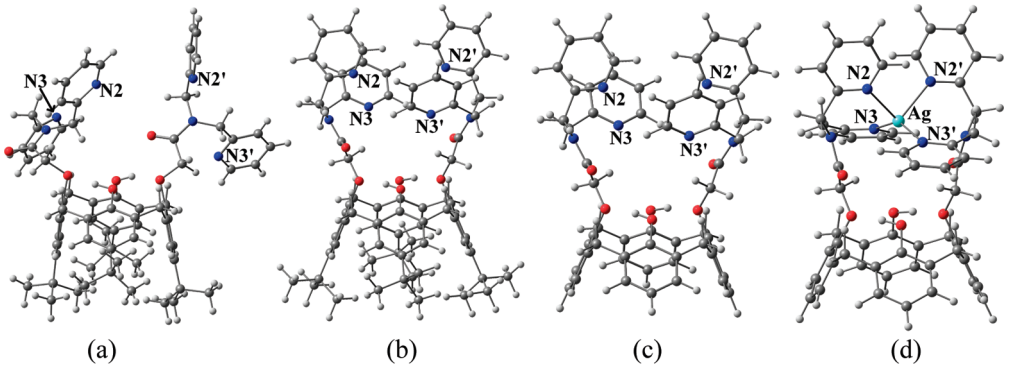

FIGURE 10. (a) Molecular structure of L from single crystal XRD, (b) L optimized through B3LYP/6-31G, (c) L′ optimized through B3LYP/6-31G, and (d) DFT optimized structure of [Ag-L′]. The bond distance (Å) and bond angles (deg) in the coordination sphere are Ag−N2 = 2.517, Ag−N3 = 2.326, Ag−N2′ = 2.517, Ag−N3′ = 2.326 Å and N2−Ag−N3 = 109.7, N2−Ag−N2′ = 98.9, N2−Ag−N3′ = 91.8, N3−Ag−N2′ = 91.8, N3−Ag−N3′ = 147.1, N2′−Ag−N3′ = 109.7°.

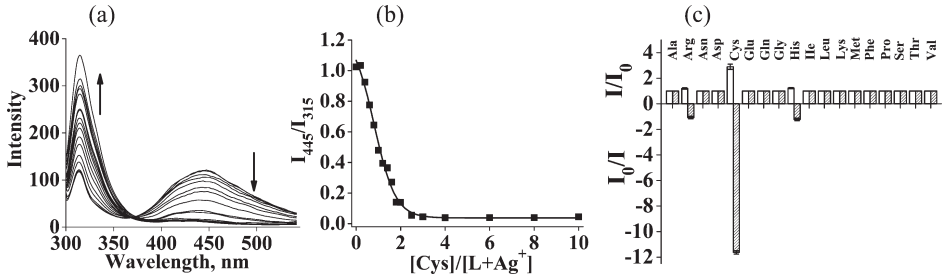

FIGURE 11. (a) Fluorescence spectral traces obtained during the titration of [L+Ag$^+$] with cysteine, (b) plot of relative fluorescence intensity (I_{445}/I_{315}) versus mole ratio of cysteine, and (c) histogram representing the effect of various amino acids on the fluorescence behavior of [L+Ag$^+$]. Filled columns = 445 nm, open columns = 315 nm.

compared to the crystal structure (Supporting Information S04). As a result of this, the inter-arm N···N distances are shortened from 5.1−8.9 Å to 4.7−5.5 Å, and intra-arm N···N distances are shortened from 4.9−5.4 Å to 3.73 Å; thus the arms are well poised for metal ion binding in the optimized L. The conformational changes of the arms are exactly same in both L and L′ (Figure 10, Supporting Information S04), and hence their coordination features are exactly same.

To study the binding characteristics of Ag^+, a starting model was generated by taking the DFT optimized L′ and placing the silver ion well above the core of pyridyl moieties at a non-interacting distance. This model was then optimized initially using HF/3-21G level of calculations, and the output structure from this was taken as input for DFT calculations performed using B3LYP with SDDAll basis set for Ag^+ and 6-31+G(d) for all other atoms in the complex. The optimized complex of Ag^+ with L′ at this stage showed a distorted tetrahedral geometry around Ag^+ where all four pyridyl nitrogens are bonded to the central ion with Ag−N distances of 2.326 and 2.517 Å (Figure 10, Supporting Information S04). These Ag−N distances are comparable with the experimental ones reported in the literature.[25] However, the geometry about Ag^+ is significantly distorted by exhibiting coordination angles in the range 91.8−147.1°.

(25) Munakata, M.; Wen, M.; Suenaga, Y.; Kuroda-Sowa, T.; Maekawa, M.; Anahata, M. *Polyhedron* **2001**, *20*, 2321.

B. Secondary Sensor Behavior of [L+Ag$^+$] and Selective Recognition of Cys among Naturally Occurring Amino Acids. Since L recognizes Ag^+ ratiometrically, the utility of [L+Ag$^+$] complex toward selective recognition of amino acid has been studied so that this complex can act as a secondary sensor.

Fluorescence Titration. The chemosensing ensemble used in these titrations was prepared *in situ* by mixing L and Ag^+ in a 1:2 ratio. Out of 20 amino acids studied for their interaction, only Trp and Tyr did not yield interpretable results owing to their strong emission that overlaps with the emission of L. The chemosensing mixture was titrated with all of the remaining naturally occurring 18 amino acids, where the fluorescence spectrum of [L+Ag$^+$] is altered only in the presence of Cys and not with the other 17 amino acids. During the titration of [L+Ag$^+$] with Cys, the emission band at 315 nm enhances and that observed at 445 nm quenches. This is exactly reverse to what happens when L is titrated with Ag^+, as reported in this paper (Figure 2), indicating that the Ag^+ is being removed from the complex by Cys to release free L (Figure 11) and thus the recognition of Cys by [L+Ag$^+$] complex as a secondary sensor. The release of L in the titration of Cys is followed by the formation of Cys complex of Ag^+ as it can form a stable complex with the thiol functionality. The necessity of -SH function and the formation of a Cys complex of Ag^+ were further proven on the basis of the emission studies performed on control molecular systems as reported in this paper. The detection limit of Cys by [L+Ag$^+$] complex has been found to be 514 ppb (Supporting Information, S05).

Titration with Control and Analogous Molecules. Since fluorescence changes occur only in the presence of Cys and not with the other amino acids, the role of the -SH function in Ag^+ binding was further confirmed by studying the fluorescence response of [L+Ag^+] with different sulfur-containing systems, *viz*., cysteine ethyl ester, cysteamine, glutathionine reduced (GSH), and glutathionine oxidized (GSSG) (Figure 12). All of these, except GSSG, exhibited changes in the fluorescence owing to the presence of the -SH functionality, whereas in GSSG the -SH is oxidized to -S-S-. Even Met does not show changes in the fluorescence owing to the presence of R-S-Me and not the -SH function. This experiment clearly suggests that Ag^+ mainly interacts through the -SH function of cysteine, and hence the [L+Ag^+] chemoensemble acts as a sensor for the thiol functionality.

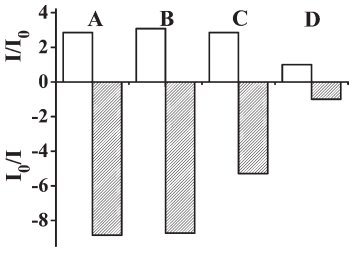

FIGURE 12. Histogram representing the enhancement and quenching fold exhibited by sulfur-containing (*viz*., -SH and -S-S-) molecules, where A = cysteine ethyl ester, B = cysteamine, C = glutathionine reduced (GSH), and D = glutathionine oxidized (GSSG). Filled and open columns correspond to 445 and 315 nm emission bands, respectively.

ESI MS Titration of [L+Ag^+] with Cys. To provide further proof for the release of L and the formation of a Cys complex of Ag^+, ESI MS titration was carried out. The spectrum exhibited two major *m*/*z* peaks (Figure 13). Whereas the peak observed at 240.2 is assignable to $[2Cys + 2Ag + Na - H]^{2+}$, that observed at 1128 is assignable to $[L + H]^+$. The first peak is from the Ag^+ complex of Cys, and the second peak is from simple L. All this clearly supports the release of L as well as the formation of the Ag^+ complex of Cys, i.e., {[L+Ag^+] + Cys → L + [Cys+Ag^+]}. Even the absorption spectral studies clearly demonstrate the release of L when Cys is added to [L+Ag^+] (Supporting Information, S06).

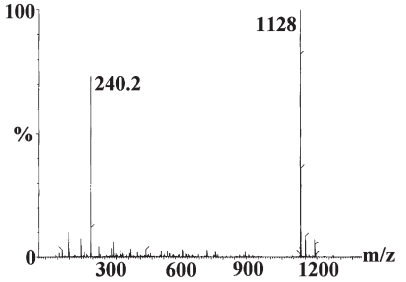

FIGURE 13. ESI mass spectrum obtained in the titration of [L+Ag^+] with Cys.

^{1}H NMR Titration of [L+Ag^+] with Cysteine and Cysteamine. The release of L and the formation of the complex of Ag^+ have been further proven through ^{1}H NMR titration carried out between [L+Ag^+] and Cys/cysteamine. The titration of [L+Ag^+] with Cys could not be continued beyond 1 equiv owing to precipitation (Supporting Information, S07); therefore, the detailed titrations were carried out using cysteamine instead of Cys, as the fluorescence behavior of both of these was found to be same. During the titration, as the concentration of cysteamine increases, the proton signals of bridged-CH_2, -OCH_2, -NCH_2, pyridyl, and lower rim phenolic-OH are shifted and moved toward simple L (Supporting Information, S07). Quantitative changes observed in the chemical shift can be seen from the plots given in Figure 14. Thus it has been found that cysteamine removes Ag^+ from the binding core of calix[4]arene using its -SH function, resulting in the recovery of simple L from the [L+Ag^+]. On the other hand the formation of the Ag^+ complex with Cys has been identified based on ESI MS.

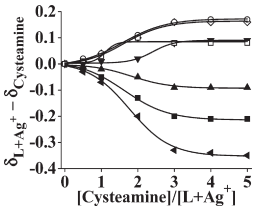

FIGURE 14. (a) Cysteamine-induced chemical shifts $\Delta\delta$ ($\Delta\delta = \delta_{(L+Ag^+}$+cysteamine $- \delta_{(L+Ag^+)}$) observed with different protons of L at various mole ratios of [cysteamine]/[L+Ag^+] as noted in Supporting Information, S07. For symbols refer to Figure 5.

TEM Studies. To determine whether the release of L from the reaction of [L+Ag^+] with Cys is reflected in their nanostructural features, TEM studies were performed with L, [L+Ag^+], and {[L+Ag^+]+Cys}, and the corresponding micrographs and particle size distributions are shown in Figure 15. The micrographs show spherical particles in the case of L. The smaller size particles are in the range of 90−150 nm, whereas the bigger clusters have diameters of 180−270 nm. The interconnectivity present in these particles is similar to that observed in case of the complexation of Hg^{2+} with amide-linked benzimidazole-1,3-di-derivative of calixarene as reported by us recently.[24] When $AgClO_4$ is added to L, the size of the particles is reduced drastically to 15−35 nm and the shape is changed to nonspherical, indicating the complexation of L with Ag^+ where the complex possessing silver ions exhibits dark spots. Thus, both the size and shape of the particles differ between L and [L+Ag^+], suggesting that it is possible to identify the complex formation between L and Ag^+ by using nanostructural features.

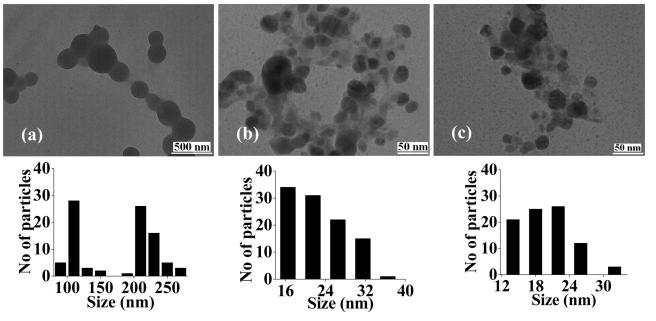

FIGURE 15. TEM images of (a) L, (b) [L+Ag^+], and (c) {[L+Ag^+]+Cys} and their particle size distribution plots (bottom). Number of particles analyzed ranges from 100 to 150 in each case.

However, the micrographs also show background images corresponding to the unreacted $AgClO_4$. Upon addition of Cys to the complex, the micrographs are filled with particles arising from L, [L+Ag^+], $AgClO_4$, and [Cys·Ag^+] complex. Therefore, it is difficult to clearly distinguish the particles of L alone from all of these because the particles containing the Ag^+ dominate as dark spots, and hence the lighter spots expected from L cannot be easily distinguished as these are buried in the background. (Supporting Information S08)

Dynamic Light Scattering (DLS) Studies. In DLS, all of the species have shown solvo-dynamic diameters of more than 10 μm. The simple ligand L is shown to have an average diameter much higher than that of its [L+Ag^+] complex as well as that observed from the reaction mixture of {[L+Ag^+] + Cys}. The trend observed in solvo-dynamic diameters is in line with the particle size distribution of the individual species observed in TEM (Supporting Information, S09).

C. INH Logic Gate Properties of L with Ag^+ and Cys. In the present case, the logic gate properties of L have been studied using two input signals as Ag^+ and Cys, respectively, by monitoring the emission of L at 445 nm (Figure 16). From the perspective of logic functions, the emission of L has been determined only by the presence of single input, *viz*., Ag^+, and not with the cysteine, as Cys is insensitive to L. This means that the emission of L is switched on only in the presence of Ag^+ (25 fold fluorescence enhancement of 445 nm band of L) and in the absence of Cys. Under the conditions where Ag^+ is absent and Cys is present, no emission is observed in the 445 nm band of L (Supporting Information, S10). Similarly in the presence of 2 equiv of Ag^+ and Cys, the fluorescence emission of L at 445 nm was quenched and no significant output signal was observed. From these studies, it has been found that L can be used as a INHIBIT (INH) logic gate toward Ag^+ in the absence of Cys by observing the emission at 445 nm. The truth table and the pictorial representation for the corresponding INH are given in Figure 16.

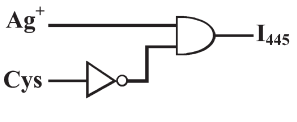

Ag^+	Cys	I_{445}
0	0	0
0	1	0
1	0	1
1	1	0

FIGURE 16. (a) INH logic gate represented using a conventional gate notation; an active output signal is obtained when Ag^+ = 1 and Cys = 0. (b) Truth table for the INH logic gate; Ag^+ and Cys are inputs to the system; I_{445} is the output signal of L at 445 nm.

Conclusions and Correlations

A structurally characterized lower rim 1,3 diamide-bis-(2-picolyl)-derivative of calix[4]arene (L) exhibits high selectivity toward Ag^+. The selectivity has been demonstrated by fluorescence, absorption, and ESI MS spectroscopy. Interaction of Ag^+ with L enhances the fluorescence emission at 445 nm and quenches the fluorescence at 315 nm, thus exhibiting a ratiometric behavior. L is sensitive and selective toward Ag^+ over nine other biologically important ions studied, *viz*., Na^+, K^+, Mg^{2+}, Ca^{2+}, Mn^{2+}, Fe^{2+}, Co^{2+}, Ni^{2+}, and Zn^{2+}, as demonstrated by individual as well as competitive metal ion titrations. L can detect up to 450 ppb by switch-on fluorescence at 445 nm; thus L is a ratiometric primary sensor for Ag^+. The necessity of the pyridyl moieties and the calix[4]arene platform in the recognition of Ag^+ has been demonstrated by comparing the fluorescence results obtained from several control molecules.

Whereas the fluorescence and absorption spectroscopy provided information for the formation of 1:1 complex between Ag^+ and L, *viz*., [LAg^+], the ESI MS confirmed the same unambiguously by exhibiting an isotopic peak pattern for the presence of silver in the complex. The complex formation between L and Ag^+ has been further followed by measuring ^{1}H NMR spectra as a function of added silver perchlorate concentration. Comparison of the changes observed in the chemical shifts of different protons, in terms of downfield and upfield, suggests Ag^+ binding in the pyridyl-nitrogen core (N_4 core) associated with some conformational changes in the calixarene platform. It has been demonstrated by transmission electron microscopy that the nanostructural features of L and its complex of Ag^+ differ substantially to differentiate the complex from that of simple L.

Therefore, the silver-binding capabilities of the nitrogen-binding core of pyridyl moieties available in L has been examined by computational calculations at the DFT level. The arms are found to be quite farther apart in the crystal structure of L as can be judged from the intra- and inter-arm N···N distances. Therefore, the binding of metal ions can take place only when considerable dihedral changes take place particularly in the arms of L. Indeed the computational calculations performed on L (or its shorter version, L′) in the presence of Ag^+ clearly demonstrated substantial changes in the dihedral angles. Comparison of the orientation of the arms and the binding cores present in the crystal structure of L, the optimized structure of L, and its Ag^+ complex clearly suggest that the arm undergoes conformational changes along with some rotation about the pyridyl moiety so as to bring all four pyridyl nitrogens in a manner to bind to the central Ag^+ in a tetrahedral fashion (Figure 17). The tetrahedral geometry observed about Ag^+ is highly distorted as can be judged on the basis of the wide range (91.8−147.1°) of coordination sphere angles observed.

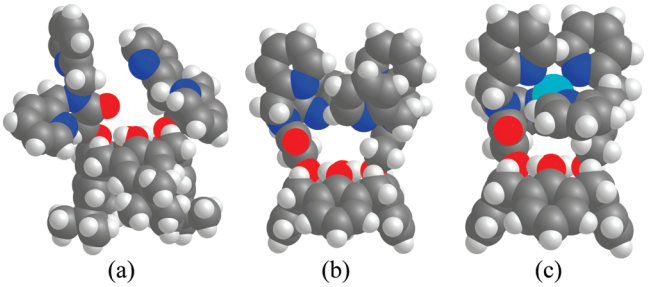

FIGURE 17. Space-filling model for (a) molecular structure of L from XRD, (b) L′ optimized at DFT (B3LYP/6-31G), and (c) [L′+Ag^+] optimized at DFT {B3LYP with mixed basis set SDDAll(Ag) and 6-31+G(d) for other atoms}. Ag^+ is in cyan.

The *in situ* prepared silver complex of L, *viz*., [L+Ag^+], was able to detect Cys ratio-metrically in a manner exactly reverse to what happens when Ag^+ is added to L in fluorescence spectroscopy. Thus, upon addition of Cys to [L+Ag^+], the 445 nm band intensity decreases and that of the 315 nm band increases, suggesting the release of L from the silver complex. The release of L has also been further proven on the basis of NMR titration. The present studies also demonstrate the

necessity of the -SH function in removing the Ag^+ from its complex of L based on several analogous and control molecules. The removal of Ag^+ by cysteine (or other -SH molecules) and the formation of a Ag^+ complex of Cys has been proven on the basis of ESI mass spectrometry. Thus the *in situ* generated [L+Ag^+] complex selectively recognizes Cys among the naturally occurring amino acids to a lowest concentration of 514 ppb, and hence L acts as secondary sensor toward Cys. The characteristic changes observed in the fluorescence spectroscopy during the sensing of Ag^+ as well Cys are represented schematically in Scheme 3 to express the primary and secondary sensor properties of L.

SCHEME 3. Schematic Representation of the Primary and Secondary Sensing Properties of L

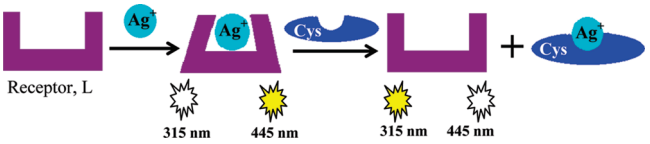

The INH logic gate has been generated by choosing Ag^+ and Cys as inputs and by monitoring the output signal at 445 nm that originated from the excimer emission of L in the presence of Ag^+. Thus L is a potential primary sensor toward Ag^+ and is a secondary sensor toward Cys, and both act ratiometrically.

Experimental Section

All the perchlorate salts, *viz*., $Mn(ClO_4)_2 \cdot 6H_2O$, $Fe(ClO_4)_2 \cdot xH_2O$, $Co(ClO_4)_2 \cdot 6H_2O$, $Ni(ClO_4)_2 \cdot 6H_2O$, $Cu(ClO_4)_2 \cdot 6H_2O$, $Zn(ClO_4)_2 \cdot 6H_2O$, $Ag(ClO_4) \cdot xH_2O$, $NaClO_4 \cdot H_2O$, $KClO_4$, $Ca(ClO_4)_2 \cdot 4H_2O$, and $Mg(ClO_4)_2 \cdot 6H_2O$, were procured from Sigma Aldrich Chemical Co., USA. All solvents used were dried and distilled by usual procedures immediately before use. Distilled and deionized water was used in the studies. The synthesis procedures and the characterization data of all molecules used in this paper are given in Supporting Information S03. Original NMR spectra of all these molecules are given in Supporting Information S03. The details of the instruments used for all studies are discussed in Supporting Information S11.

Ligand L. A suspension of bis(2-picolyl)amine (0.59 g, 2.96 mmol) and Et_3N (0.55 g, 5.43 mmol) was stirred in dry THF (30 mL) under argon atmosphere. Diacid chloride **4** (1.08 g, 1.35 mmol) in dry THF (30 mL) was added dropwise to this reaction mixture. Immediately, a yellowish precipitate was formed, and stirring was continued for 48 h at room temperature. After filtration, the filtrate was concentrated to dryness. A yellow solid was obtained that was extracted with $CHCl_3$ and washed with water and then with brine, and the organic layer was dried with anhydrous $MgSO_4$. Filtrate was concentrated to dryness and purified by column chromatography to give L as white solid. Yield (35%, 0.52 g). Anal. Calcd for $C_{72}H_{82}N_6O_6 \cdot C_2H_5OH$: C, 75.74; H, 7.56; N, 7.16. Found: C, 75.18; H, 7.34; N, 7.34. FTIR (KBr, cm^{-1}): 1641 ($\nu_{C=O}$), 3394 (ν_{OH}). ^{1}H NMR ($CDCl_3$, δ ppm): 0.93 (s, 18H, $C(CH_3)_3$), 1.27 (s, 18H, $C(CH_3)_3$), 3.27 (d, 4H, Ar-CH_2-Ar, J = 13.14 Hz), 4.34 (d, 4H, Ar-CH_2-Ar, J = 13.14 Hz), 4.71, 4.94 (s, 8H, NCH_2), 4.97 (s, 4H, OCH_2), 6.76 (s, 4H, Ar-**H**), 7.02 (s, 4H, Ar-**H**), 7.04 (t, 2H, Py-**H**, J = 6.40 Hz), 7.13 (t, 2H, Py-H, J = 6.42 Hz), 7.25 − 7.27 (m, 2**H**, Py-**H**), 7.40 (d, 2H, Py-**H**, J = 7.90 Hz), 7.51−7.58 (m, 6H, Py-**H** and O**H**), 8.41 (d, 2H, Py-**H**, J = 4.88 Hz) 8.52 (d, 2H, Py-**H**, J = 4.88 Hz). ^{13}C NMR ($CDCl_3$, 100 MHz δ ppm): 31.1, 31.8 ($C(CH_3)_3$), 31.9 (Ar-CH_2-Ar), 33.9, 34.0 ($C(CH_3)_3$), 51.4, 52.2 (NCH_2), 74.5 (OCH_2CO), 122.2, 122.3, 122.5, 125.1, 125.7, 127.9, 132.7, 136.7, 136.9, 141.3, 147.1, 148.9, 149.9, 150.8, 156.4, 157.3 (Py-*C* and calix-Ar-**C**), 169.2 (**C**=O). m/z (ES-MS) 1127.78 ([M]$^+$ 70%), 1128.80 ([M + H]$^+$ 40%,).

Solutions for Spectroscopy. The fluorescence and absorption titrations were carried out in methanol. The concentration of L and its reference molecules were kept constant at 10 μM for the fluorescence titrations and at 20 μM for the absorption titrations. The amino acids were dissolved in 500 μL of water and diluted further using methanol to get the required concentration. ^{1}H NMR titrations, *viz*., Ag^+ and cysteamine with L (0.011 M), were carried out in DMSO-d_6 (400 μL) except for the cysteine titration, where the amino acid was dissolved in D_2O (200 μL).

Solutions and Sample Preparation for TEM and DLS Studies. Ligand L and silver perchlorate solutions were made in methanol. Cys solution was made by dissolving the amino acid in ~500 μL deionized water and then the volume was made up by methanol. The final concentration of the solutions was kept ~6×10^{-4} M. TEM and DLS studies of L were carried out by using a solution of 50 μL in 3.0 mL of methanol, which results in 10 μM as also used in case of fluorescence studies. For the silver complexation studies 50 μL of L was mixed with 100 μL of Ag^+. Similarly for the reaction with Cys, 100 μL of Cys was added to the silver complex. Different sample blocks for TEM were made by placing 20−30 μL of the sonicated (15 min) sample solution on the copper grid and allowing it to dry in air at room temperature.

Acknowledgment. C.P.R. acknowledges the financial support by DST, CSIR, and BRNS-DAE. R.J. thanks UGC, and A.A. thanks CSIR for their research fellowships. We thank SAIF and CRNTS, IIT Bombay for TEM and DLS measurements.

Supporting Information Available: Single crystal X-ray structural information (S01), minimum detection limit (S02 and S05), synthesis and characterization (S03), computational data (S04), absorption data (S06), ^{1}H NMR titration data (S07), TEM and DLS data (S08 and S09), fluorescence titration data (S10), and instrumental details (S11). This material is available free of charge via the Internet at http://pubs.acs.org.